Supporting Information

Nosavanh et al. 10.1073/pnas.1420978112

SI Materials and Methods

Materials. Antibodies used in this study included mouse anti-acetylated tubulin (1:1,000; Sigma), goat anti-Gli2 (1:1,000 for Western blot, 1:50 for immunofluorescence; R&D Systems), goat anti-Gli3 (1:1,000 for Western blot, 1:50 for immunofluorescence; R&D Systems), rabbit anti-Smo (1:50; Santa Cruz), rabbit anti-Sufu (1:2,000; Santa Cruz), rabbit anti-PPARγ (1:100; Abcam), rabbit anti-C/EBPβ (1:50; Abcam), sheep anti-PRDM16 (1:500; R&D Systems), rabbit anti-UCP1 (1:50; Abcam), rabbit anti-aP2 (1:300; Abcam), mouse anti-Actin, α Smooth Muscle (1:500; Sigma), rabbit anti-Ki-67 (1:250; Abcam), rabbit anti-Desmin (1:200; Abcam), mouse anti-Myosin Heavy Chain (1:25; R&D Systems), mouse anti-Myogenin (1:100; Thermo Scientific), mouse anti–alpha-Tubulin (1:2,000; Sigma), rabbit anti-GFP (1:500; Abcam), mouse anti-human COUP-TFII (1:100; R&D Systems), donkey anti-mouse AlexaFluor 594 (1:2,000; Invitrogen), donkey anti-rabbit AlexaFluor 488 and 594 (1:2,000; Invitrogen), donkey anti-goat AlexaFluor 488 (1:2,000; Invitrogen), donkey anti-mouse HRP (1:2,000; The Jackson Laboratory), donkey anti-goat HRP (1:2,000; The Jackson Laboratory), donkey anti-rabbit HRP (1:2,000; The Jackson Laboratory), biotinylated goat anti-rabbit IgG (1:1,000; Vector Laboratories), biotinylated goat anti-mouse IgG (1:1,000; Vector Laboratories), biotinylated rabbit anti-sheep IgG (1:1,000; Vector Laboratories), and SA-HRP (1:100; Vector Laboratories). Small molecules used in this study included SAG (1 μM, 200 nM used for experiments in Fig. S6*B*; Calbiochem), cyclopamine hydrate (10 μM; Sigma), SANT-1 (10 μM; Sigma), and recombinant mouse Sonic Hedgehog (Shh C25II, 1 μg/mL; R&D Systems). SAG, cyclopamine, and SANT1 were dissolved in DMSO whereas Shh was dissolved in PBS. Plasmids used included pMSCV-COUP-TFII constructs, which were kindly provided by Evan Rosen (Harvard University, Cambridge, MA). The 8XGliBS-Luc, pRL-TK, and pcDNA3-Gli1, Gli2, and Gli3 expression constructs were kindly provided by Pao-Tien Chuang (University of California, San Francisco). Other plasmids used were pCL-ECO (Addgene plasmid no. 12371), pBABE-neo-LargeTcDNA (Addgene plasmid no. 1780), pLKO.1 (Addgene plasmid no. 10878), psPAX2 (Addgene plasmid no. 12260), and pMD2.G (Addgene plasmid no. 12259).

Animals. Mouse husbandry and embryo collection procedures were approved by the Institutional Animal Care and Use Committee at Baylor College of Medicine. The *aP2-Cre*, *Ptch1*, *R26-SmoM2*, and *R26R* (*R26R-LacZ*) reporter mice were obtained from The Jackson Laboratory. The $Ptch1^{flox}$ mice were kindly provided by Pao-Tien Chuang (University of California, San Francisco). Mice were maintained in a mixed genetic background and genotyped as previously described (1–3). The *aP2-Cre* mice were genotyped using primer OCH53 (5′CTAAGTCCAGTGATCATTGCCAGGGA3′) and primer OCH54 (5′CCGGCAAACGGACAGAAGCA3′). The *R26R* reporter mice were genotyped using primer OCH328 (5′GCATCGAGCTGGGTAATAAGCGTTG 3′) and primer OCH329 (5′CCAGACCAACTGGTAATGGTAGCGAC3′).

Cell Lines. The brown-preadipocyte cell line FVB-C3 was kindly provided by Qiang Tong (Baylor College of Medicine). These cells were originally obtained from the laboratory of Ronald Kahn (4). HEK 293T cells were kindly provided by Yu-Xiang Sun (Baylor College of Medicine).

Embryonic Brown-Preadipocyte Cell-Line Generation and Differentiation. Primary brown preadipocytes (stromal-vascular fraction) were isolated by collagenase [collagenase B (Roche), 1 mg/mL, 30 min at 37 °C] digestion of interscapular BAT from E16.5 or E18.5 WT and *aP2-Cre; SmoM2* mouse embryos. DMEM (Invitrogen) and Pen/Strep (Invitrogen) were added to the digested tissues, followed by centrifugation at 500 × *g* for 5 min to pellet the stromal-vascular fraction. The floating fraction contained the primary mature brown adipocytes. Cells from the stromal-vascular fraction were subsequently immortalized using pBABE-neo-LargeTcDNA following a previously described method (5). To induce brown preadipocytes to differentiate, we first cultured these cells in growth medium containing DMEM (Invitrogen), 10% (vol/vol) FBS (Sigma), and Pen/Strep (Invitrogen) until cells reached 100% confluence. The cells were then incubated in growth medium supplemented with 2–4 nM recombinant human Bmp7 (Prospec), 1 μM rosiglitazone (Cayman), 5 mg/mL insulin (Sigma), and 1 nM T3 (Sigma) for 2 d. After induction, these cells were maintained in growth medium supplemented with 5 mg/mL insulin and 1 nM T3 for another 8 d (Fig. S6*A*). To activate the thermogenic program and measure metabolic gene expression, differentiated cells were incubated with 10 μM Isoproterenol (Iso) for 6 h. Cells were stained with either Oil Red O or BODIPY493/503 at the end of the culture period.

Embryo Processing and Histology. For paraffin embedding, embryos from various embryonic stages were fixed in 4% paraformaldehyde at 4 °C overnight, dehydrated in 100% ethanol, and cleared in toluene solution before embedding in paraffin. For frozen embedding, brown adipose tissues were fixed in 4% paraformaldehyde at 4 °C overnight, cryopreserved in 30% (wt/vol) sucrose, and embedded in O.C.T. compound (Tissue-Tek). Paraffin-embedded embryos were sectioned at 6-μm thickness for histological analysis and immunohistochemistry. Frozen embedded brown adipose tissues were sectioned at 10-μm thickness for immunofluorescence. H&E staining was performed using standard procedures. H&E-stained sections were imaged by using a DS-Fi1 camera connected to a Nikon Eclipse 80i stereomicroscope, and images were processed using NIS Elements AR 3.2 Nikon imaging software. For quantification, H&E-stained brown adipose tissues were measured by outlining the brown adipose tissue area on the section using NIS Elements AR 3.2 software. Statistical significance was determined by the nonparametric Mann–Whitney method using Prism 6 software. For whole-tissue imaging, E18.5 embryonic tissues were dissected in PBS and imaged using a DS-Fi1 camera connected to a Nikon SMZ1500 stereomicroscope. Images were processed using NIS Elements BR 3.2 Nikon imaging software.

Immunofluorescence. Frozen brown adipose tissue sections or E18.5 embryo sections were rinsed with PBS twice, blocked with 3% (vol/vol) H_2O_2 solution for 30 min, and incubated with blocking solution for 1 h at room temperature before applying primary antibody (anti-acetylated tubulin or anti-GFP) at 4 °C overnight. Secondary antibody (Alexa-594) was applied to the sections for 45 min, and then they were rinsed in PBS three times (5 min each). Finally, tissue sections were incubated with DAPI (Sigma) for 10 min to counterstain the nuclei. Immunofluorescence of cells was performed as previously described (6). Briefly, cells were rinsed in PBS twice and fixed in 4% paraformaldehyde for 10 min. After fixation, cells were washed in PBS or PBS with 50 mM glycine three times and permeabilized in 0.2–0.3% Triton X-100 for 15 min at room temperature. To block nonspecific staining, cells were incubated in blocking solution [5% (vol/vol) sheep serum, 0.2% BSA, 0.01% Triton X-100 in PBS] for 1 h and

then incubated with primary antibody in PBS at 4 °C overnight. Cells were then washed in PBS and incubated with secondary antibody for 1 h at room temperature. Cells were counterstained with DAPI for 10 min before mounting. Cells/tissues were imaged by using a CoolSNAP$_{ES}^2$ camera connected to a Nikon Eclipse 80i stereomicroscope, and images were processed using NIS Elements AR 3.2 Nikon imaging software.

β-Galactosidase Staining. β-Gal staining of E18.5 embryonic tissues was performed as previously described (7). Briefly, embryonic tissues were dissected in PBS and fixed in β-gal fix solution [2% (wt/vol) paraformaldehyde, 0.2% glutaraldehyde in PBS] for 6 h or more at 4 °C. After fixation, tissues were rinsed in PBS for 30 min and stained from 3 h to overnight at room temperature in staining solution (1 mg/mL β-gal, 5 mM ferricyanide, 5 mM ferrocyanide, 0.1% deoxycholate, 0.2% Nonidet P-40, 2 mM $MgCl_2$, 20 mM Tris, pH 7.4, in PBS). After staining, the tissues were rinsed in PBS for 30 min and fixed in 4% paraformaldehyde at 4 °C overnight. β-Gal–stained tissues were imaged by using a DS-Fi1 camera connected to a Nikon SMZ1500 stereomicroscope, and images were processed using NIS Elements BR 3.2 Nikon imaging software. After images were taken, these tissues were dehydrated for embedding in paraffin. Paraffin-embedded tissues were sectioned at 8-μm thickness and counterstained with eosin (0.5% eosin Y; Sigma). β-Gal–stained slides were imaged by using a DS-Fi1 camera connected to a Nikon Eclipse 80i stereomicroscope, and images were processed using NIS Elements AR 3.2 Nikon imaging software.

Immunohistochemistry. Tissue slides were first dewaxed in xylene twice (5 min each) and rehydrated with 100% ethanol twice (5 min each), 95% ethanol twice (5 min each), and PBS twice (2 min each). To block endogenous peroxidases, slides were incubated in 3% H_2O_2 for 30 min at room temperature and then rinsed in PBS three times (5 min each). Slides were incubated in blocking solution (5% sheep serum, 0.2% BSA, 0.1% Triton X-100 in PBS) for 1 h at room temperature to reduce nonspecific staining and then with primary antibody at 4 °C overnight. Slides were then rinsed in TNT solution (0.1 M Tris pH 7.5, 0.15 M NaCl, 0.025% Tween 20) three times (5 min each) and incubated with anti-biotin secondary antibody diluted 1:1,000 in TNB solution (0.5% blocking reagent in TNT) for 45 min at room temperature in the dark. This step was followed by rinsing slides in TNT solution three times (5 min each) and incubating with SA-HRP diluted 1:100 in TNB for 30 min at room temperature in the dark. Slides were developed using the DAB kit (Vector Laboratories). Antigen-retrieval procedures were performed before peroxidase-blocking procedure for some of the antigens. After IHC, slides were imaged using a DS-Fi1 camera connected to a Nikon E80i stereomicroscope. Images were processed using Nikon imaging software (NIS Elements AR 3.2). For quantification, IHC images were taken at the same light setting, exposure time, and magnifications. The percentage of the area of the section that contains DAB stain was determined by using NIH ImageJ (1.47v) plugin ImmunoRatio (nuclear staining) or Nikon NIS Elements AR 3.2. (membrane staining). Brown adipose tissue sections from four WT and four *aP2-Cre; SmoM2* embryos were used for IHC. Statistical significance was determined by the nonparametric Mann–Whitney method using Prism 6 software.

Western Blots. Brown preadipocytes were treated with or without SAG for 24 h and lysed in RIPA buffer (50 mM Tris·Cl, pH 7.5, 150 mM NaCl, 5 mM EDTA, 1% Triton X-100, 0.1% SDS, 1% Na deoxycholate, and protease inhibitors). SDS/PAGE and Western blotting were performed as previously described (5).

RNA Isolation, RT-PCR, and qRT-PCR Analysis. Total RNA was first extracted by homogenizing the cell pellets with TRIzol (Invitrogen) and then purified using the RNAeasy Mini Kit following the manufacturer's instructions (Qiagen). First-strand cDNA was reverse transcribed from 1 μg of total RNA using SuperScript III Reverse Transcriptase with oligo(dT)20 primers (Invitrogen). qPCR were performed in triplicate using 250 ng of first-strand cDNA for each amplification. PCR reactions were performed using Platinum SYBR Green qPCR SuperMix UDG (Invitrogen). mRNA expression of target genes, normalized to beta-actin expression, was determined using the $\Delta\Delta^{-}C_t$ method. Regular PCR reactions were performed according to standard PCR procedures using Taq polymerase (Invitrogen). Primer sequences used for RT-PCR are listed in Table S1. Primer sequences used for qRT-PCR are listed in Table S2. For qRT-PCR, statistical significance was determined by either the Student's *t* test or one-way ANOVA.

BODIPY 493/503 and Oil Red O Staining. Brown adipocytes were rinsed twice in PBS, fixed in 4% paraformaldehyde for 30 min, and stained with BODIPY 493/503 diluted in PBS (1:1,000; Sigma) for another 30 min. Cells were counterstained with DAPI for 10 min and coverslipped with mounting medium (Vector Laboratories). For Oil Red O staining, brown adipocytes were washed in PBS, fixed in 4% paraformaldehyde for 30 min, rinsed with 60% (vol/vol) isopropanol, and incubated with Oil Red O staining solution (Sigma) at room temperature for 2 h. Cells were then washed in ddH_2O and visualized. BODIPY-stained cells were imaged using a CoolSNAP$_{ES}^2$ camera connected to a Nikon Eclipse 80i stereomicroscope, and images were processed using NIS Elements AR 3.2 Nikon imaging software. Oil Red O-stained cells were imaged using a DS-Fi1 camera connected to a Nikon SMZ1500 stereomicroscope, and images were processed using NIS Elements BR 3.2 Nikon imaging software. BODIPY fluorescence intensity was quantified using NIH ImageJ (1.47v). Briefly, images saved as RGB color were converted to 16-bit monochrome files, and pixel intensities were measured for each image. For quantification of Oil Red O staining, Oil Red O was extracted from cells with 100 μL of 100% isopropanol at room temperature for 10 min. Extracted dye was then transferred to a microplate reader (Infinite PRO 200; TECAN) and quantified at an absorbance of 520 nm. Statistical significance was determined by the nonparametric Mann–Whitney method or the Kruskal–Willis method.

Retroviral Production and Generation of Stable Cell Lines. HEK 293T cells were transfected with pCL-ECO and with either pMSCV-COUP-TFII or pMSCV empty vector using Lipofectamine 2000 (Invitrogen). The retroviral supernatant was collected 72 h after transfection, filtered through a 0.45-μm syringe filter, and added, along with 8 μg/mL polybrene (Sigma), to 50–60% confluent brown-preadipocyte cells. Two days after addition of the retroviral supernatant, cells were split 1:5 and selected with 2.5 μg/mL puromycin (Sigma). A total of six clones were selected for each transfection, and stable expression of COUP-TFII was verified by Western blotting.

Lentiviral Production and Generation of Stable Cell Lines. Short hairpin RNA (shRNA) plasmids were constructed and lentiviral particles were produced following the protocol described by Moffat et al. (8). Briefly, DNA oligonucleotides were synthesized, annealed, and cloned into pLKO.1 at AgeI and EcoRI sites. The targeting sequence of mouse *COUP-TFII* was 5′ AGCTCTTGCTTCGTCTCCC 3′. Firefly luciferase shRNA (shLuc) was used as a negative control. The shRNA plasmids were cotransfected with psPAX2 and pMD2.G into 293T cells to produce viral supernatants. Then, 48 h after transfection, the culture medium was filtered through a 0.45-μm filter, and the viral supernatant was used for WT and *aP2-Cre; SmoM2* brown-preadipocyte infection. Knockdown efficiency was determined by Western blot. Oligo sequences for generation of the *COUP-TFII*

shRNA construct were as follows: OCH203, 5′ CCGGAGC TCTTGCTTCGTCTCCCACTCGAGAGGGAGACGAAGCA-AGAGCTTTTTG 3′ and OCH204, 5′ AATTCAAAAAAGC-TCTTGCTTCGTCTCCCTCTCGAGTGGGAGACGAAGCA-AGAGCT 3′. Oligo sequences for generation of the shLuc construct were as follows: OCH201, 5′ CCGGCCTTACGCTGA-GTACTTCGAGTGTGCTGTCCTCGAAGTACTCAGCGTA-AGTTTTTTTTG 3′ and OCH202, 5′ AATTCAAAAAAAA-CTTACGCTGAGTACTTCGAGGACAGCACACTCGAAGT-ACTCAGCGTAAGGCCGG 3′. Oligo sequences for generation of the *Sufu* shRNA construct were as follows: OCH318, 5′ CCGG-GAGTTGACGTTTCGTCTGAAGACTCGAGACTTCAGAC-GAAACGTCAACTCTTTTTG 3′ and OCH319, 5′ AATTCA-AAAAGAGTTGACGTTTCGTCTGAAGTCTCGAGTCTTC-AGACGAAACGTCAACTC 3′.

Luciferase Assays. A previously identified fragment (NM183261; −3,958 bp to −2,686 bp relative to the *COUP-TFII* transcriptional start site) (9) containing a potential Gli-responsive element from the *COUP-TFII* promoter was PCR-amplified from mouse genomic DNA and cloned into a pGL3-basic vector to generate the COUP-TFII reporter construct. The primers used for PCR amplification were as follows: mCOUP-TFII F1(KpnI), CTTTGGTACCCTGCCTGAGAGCTGAGCCGC and R1(XhoI), CAATCCAATCTCGAGCTCTCCACCTCTTTTCGGCCTT. For luciferase reporter assays, BAC-C4 cells were seeded in a 48-well plate 1 d before transfection. pcDNA3-Gli expression constructs, the COUP-TFII reporter construct, and a *Renilla* luciferase expression vector (pRL-TK; used as an internal control) were co-transfected with Lipofectamine 2000 (Invitrogen) at a 5:4:1 ratio. Firefly and *Renilla* luciferase activity was measured 48 h after transfection using the Dual-Luciferase Reporter Assay System (Promega) and a GloMax-Multi detection system (Promega). Results are from three independent biological replicates. Hh-pathway activity was determined by cotransfecting pcDNA3/*8xGliBS-Luc* and pRL-TK constructs into SmoM2 cells using the above-mentioned methods. Statistical significance was calculated using either the Student's *t* test or one-way ANOVA.

Chromatin Immunoprecipitation and Real-Time PCR. ChIP analyses were performed as described previously (10). Antibodies used were either anti-Gli2 antibody (ab26056; Abcam,) or control IgG (AB-105-C; R&D Systems). ChIP products were quantified by TaqMan Real-time PCR on an ABI StepOnePlus Detection System. Primer and probe sets to generate products containing the region of predicted Gli binding site (−3,167 bp to −3,159 bp) at the COUP-TFII promoter (−3,958 bp relative to the transcriptional start site) and the negative control regions are summarized in Table S3.

Statistical Analyses. The Student's *t* test and the Mann–Whitney method were used to evaluate statistical significance between two groups. One-way ANOVA and the Kruskal–Wallis method were used to evaluate statistical significance among three or more groups. Unless specified, the following applied: $^{***}P < 0.001$, $^{**}P < 0.01$, $^{*}P < 0.05$, and nonsignificant (ns), $P > 0.05$. Prism 6 software was used to perform statistical analyses and generate graphs.

1. Goodrich LV, Milenković L, Higgins KM, Scott MP (1997) Altered neural cell fates and medulloblastoma in mouse patched mutants. *Science* 277(5329):1109–1113.
2. Mak KK, Chen MH, Day TF, Chuang PT, Yang Y (2006) Wnt/beta-catenin signaling interacts differentially with Ihh signaling in controlling endochondral bone and synovial joint formation. *Development* 133(18):3695–3707.
3. Jeong J, Mao J, Tenzen T, Kottmann AH, McMahon AP (2004) Hedgehog signaling in the neural crest cells regulates the patterning and growth of facial primordia. *Genes Dev* 18(8):937–951.
4. Klein J, et al. (1999) beta(3)-adrenergic stimulation differentially inhibits insulin signaling and decreases insulin-induced glucose uptake in brown adipocytes. *J Biol Chem* 274(49):34795–34802.
5. Chen MH, et al. (2009) Cilium-independent regulation of Gli protein function by Sufu in Hedgehog signaling is evolutionarily conserved. *Genes Dev* 23(16):1910–1928.
6. Firestone AJ, et al. (2012) Small-molecule inhibitors of the AAA+ ATPase motor cytoplasmic dynein. *Nature* 484(7392):125–129.
7. Anderson JP, et al. (2004) HRC is a direct transcriptional target of MEF2 during cardiac, skeletal, and arterial smooth muscle development in vivo. *Mol Cell Biol* 24(9): 3757–3768.
8. Moffat J, et al. (2006) A lentiviral RNAi library for human and mouse genes applied to an arrayed viral high-content screen. *Cell* 124(6):1283–1298.
9. Pospisilik JA, et al. (2010) Drosophila genome-wide obesity screen reveals hedgehog as a determinant of brown versus white adipose cell fate. *Cell* 140(1):148–160.
10. Yu DH, et al. (2013) Developmentally programmed 3′ CpG island methylation confers tissue- and cell-type-specific transcriptional activation. *Mol Cell Biol* 33(9):1845–1858.

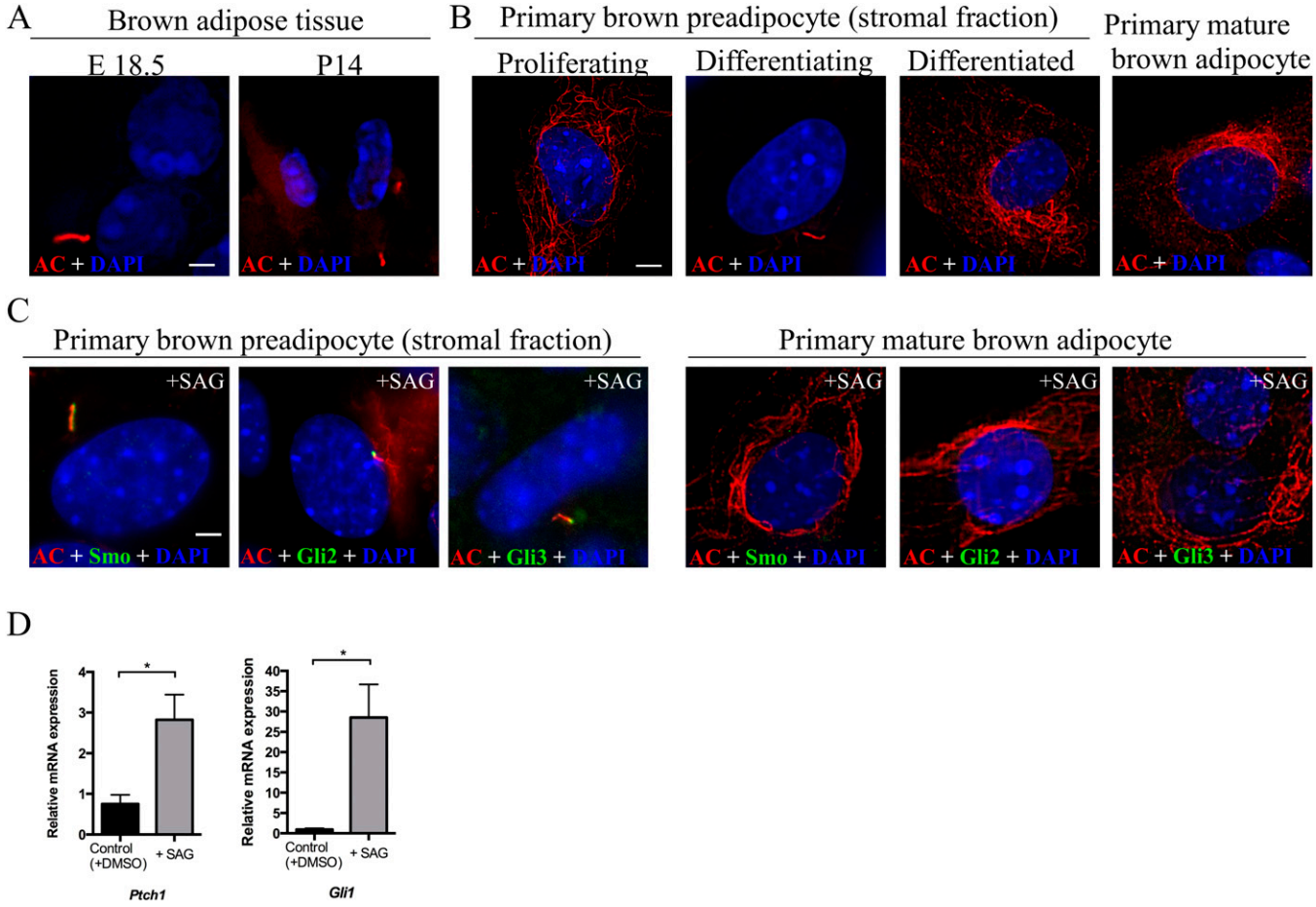

Fig. S1. Primary cilium and major Hh-pathway components are present in primary brown preadipocytes. (*A*) Immunofluorescence with anti-acetylated tubulin (AC) to detect the primary cilium was performed on frozen sections of WT BAT ($n = 3$). (Scale bar: 10 μm.) (*B*) Immunofluorescence with anti-acetylated tubulin (AC) to detect the primary cilium in proliferating, differentiating, and differentiated primary brown preadipocytes and in mature primary brown adipocytes. Proliferating preadipocytes and mature adipocytes were derived from E18.5 WT mouse embryos, and preadipocytes were induced to differentiate to obtain differentiating and differentiated cells. (Scale bar: 10 μm.) (*C*) Double immunofluorescence staining using antibodies against acetylated tubulin (red) and Hh-pathway components (Smo, Gli2, and Gli3; green) in primary brown preadipocytes and mature primary brown adipocytes derived from E18.5 WT embryos. (Scale bar: 10 μm.) (*D*) qRT-PCR analysis of *Ptch1* and *Gli1* in primary brown preadipocytes treated with SAG relative to untreated cells ($n = 3$). Data are presented as mean ± SD; $^*P < 0.05$.

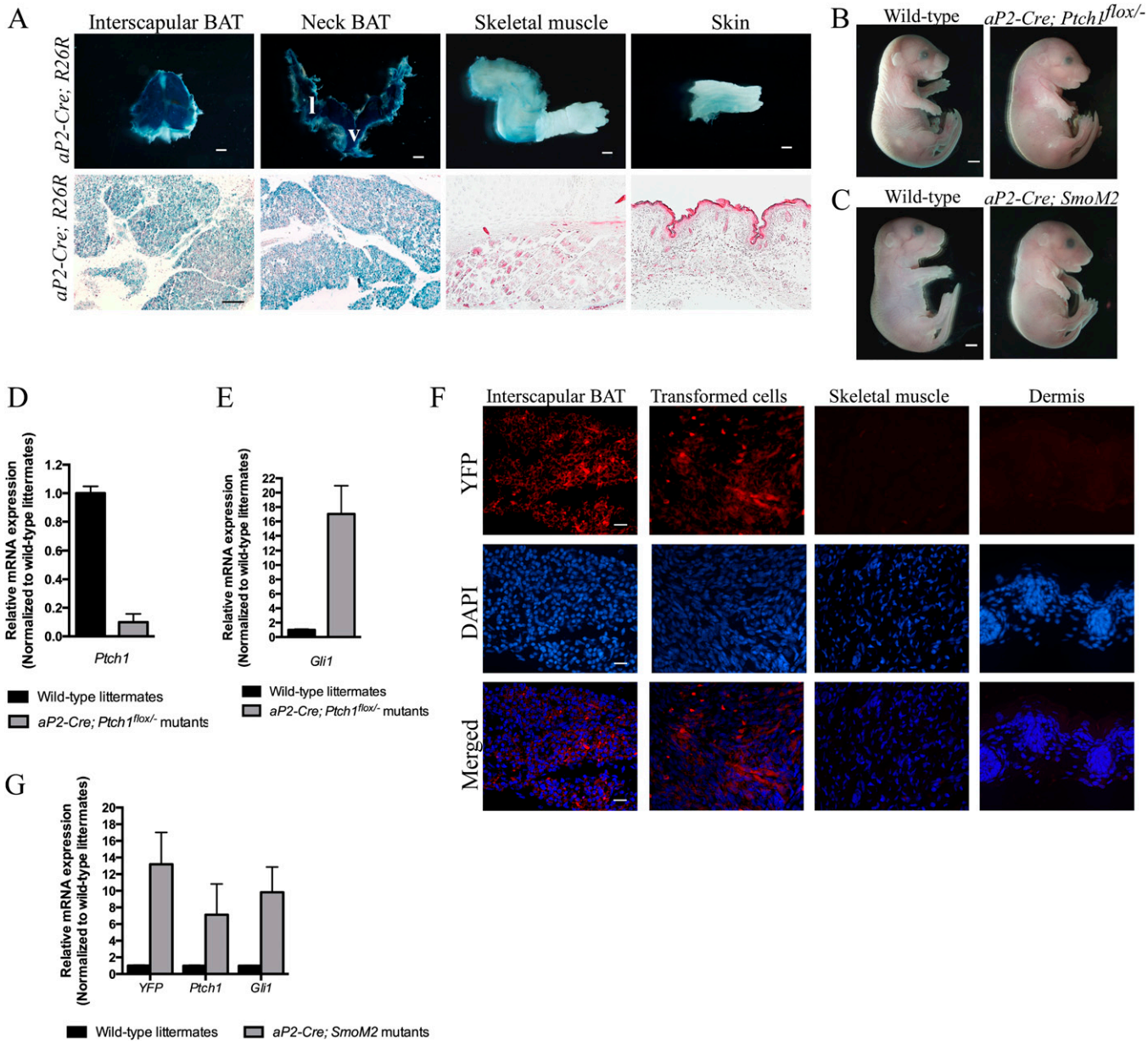

Fig. S2. *aP2*-Cre recombinase is expressed in embryonic BAT depots but not in skeletal muscle or skin and drives increased Hh-pathway activity in both *aP2-Cre; SmoM2* and *aP2-Cre; Ptch1*$^{flox/-}$ embryos. (*A*) β-Gal staining of E18.5 interscapular BAT, neck BAT (including supraclavicular and ventral neck regions), skeletal muscle (forelimb), and skin (isolated from the neck region) of *aP2-Cre; R26R* embryos (*Upper*). l, lateral; v, ventral. (Scale bar: 1,000 μm.) Sections of the corresponding β-gal–stained tissues are shown in the *Lower* panel. (Scale bar: 100 μm.) (*B*) Lateral view of E18.5 WT and *aP2-Cre; Ptch1*$^{flox/-}$ embryos. (Scale bar: 1,000 μm.) (*C*) Lateral view of E18.5 WT and *aP2-Cre; SmoM2* embryos. (Scale bar: 1,000 μm.) (*D*) qRT-PCR analysis to confirm loss of *Ptch1* transcripts in the BAT tissues isolated from the supraclavicular and ventral neck regions of *aP2-Cre; Ptch1*$^{flox/-}$ embryos. For this analysis, primers that amplify exon 2 were used because exon 2 is deleted upon Cre excision ($n = 2$) (1, 2). Data are presented as mean ± SD. (*E*) qRT-PCR analysis of *Gli1* expression in BAT tissues isolated from the supraclavicular and ventral neck regions (where transformed skeletal muscle-like cells reside) of *aP2-Cre; Ptch1*$^{flox/-}$ embryos ($n = 2$). Data are presented as mean ± SD. The expression of *Gli1* is increased in the mutants, indicating that the Hh pathway is activated in these cells. (*F*) Immunofluorescence using anti-GFP to detect SmoM2-YFP fusion protein in tissue sections of E18.5 *aP2-Cre; SmoM2* embryos. Both interscapular BAT and transformed skeletal muscle-like cells showed strong YFP staining (red color) whereas the skeletal muscle and dermis did not. (Scale bar: 25 μm.) (*G*) qRT-PCR analysis of *YFP*, *Ptch1*, and *Gli1* expression in BAT tissues isolated from the supraclavicular and ventral neck regions of *aP2-Cre; SmoM2* embryos relatives to expression in WT littermates ($n = 3$). Data are presented as mean ± SD. The expression of these Hh target genes is increased, indicating that the Hh pathway is activated in BAT cells in these embryos.

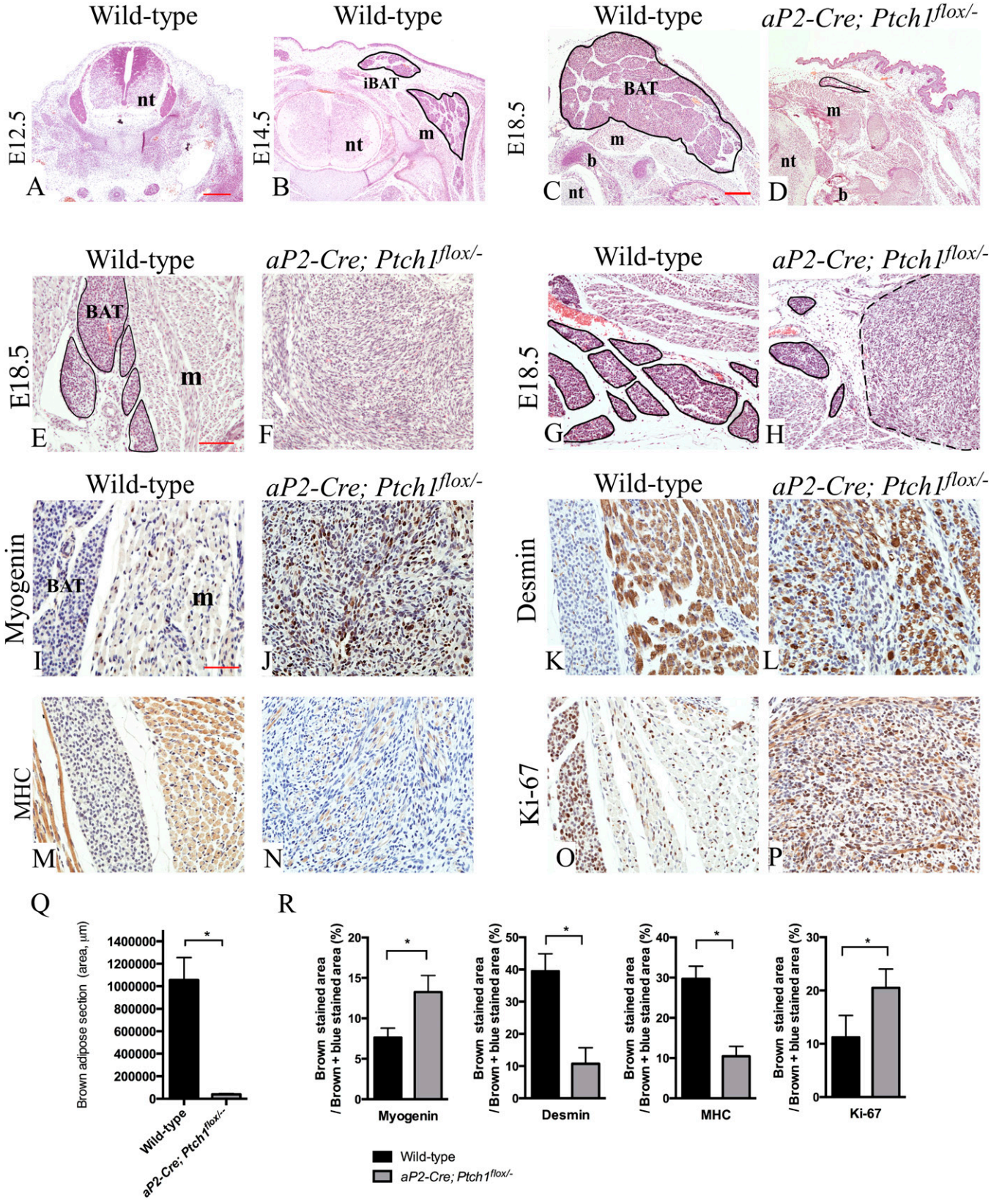

Fig. S3. BAT is nearly completely absent from *aP2-Cre; Ptch1*$^{flox/-}$ embryos and is replaced by poorly differentiated skeletal muscle in the supraclavicular and ventral neck regions. (*A* and *B*) Transverse sections of an E12.5 WT mouse embryo (*A*) and an E14.5 WT mouse embryo (*B*) at the thoracic/heart level. BAT becomes visible at E14.5 (*B*) and continues to develop until birth. Interscapular BAT (iBAT) is outlined in black. m, muscle; nt, neural tube ($n = 3$). (Scale bar: 100 μm.) (*C* and *D*) H&E-stained E18.5 WT and *aP2-Cre; Ptch1*$^{flox/-}$ mouse embryo sections containing interscapular BAT. b, bone; m, muscle; nt, neural tube. Interscapular BAT is outlined in black. (*E* and *F*) H&E staining of supraclavicular BAT in E18.5 WT and *aP2-Cre; Ptch1*$^{flox/-}$ embryos. The majority of the

Legend continued on following page

supraclavicular BAT in *aP2-Cre; Ptch1*$^{flox/-}$ embryos was replaced by poorly differentiated skeletal muscle. BAT is outlined in black. m, muscle. (*G* and *H*) H&E staining of paraffin sections of the ventral neck region of E18.5 WT and *aP2-Cre; Ptch1*$^{flox/-}$ embryos. BAT in the ventral neck was drastically reduced, and nodules (outlined with a dashed line) containing poorly differentiated skeletal muscle appeared in *aP2-Cre; Ptch1*$^{flox/-}$ embryos. (*C–H*) Images are representative of four embryos per genotype. (Scale bars: *C–H*, 100 μm.) (*I–P*) IHC of E18.5 WT and *aP2-Cre; Ptch1*$^{flox/-}$ transformed skeletal muscle using antibodies against Myogenin (*I* and *J*), Desmin (*K* and *L*), Myosin Heavy Chain (MHC) (*M* and *N*), and Ki-67 (*O* and *P*). Images are representative of four embryos per genotype. (Scale bar: 50 μm.) (*Q*) Quantitative analyses of the area of BAT observed in sections *C* and *D* from WT and *aP2-Cre; Ptch*$^{flox/-}$, embryos. Data are presented as mean ± SD; **P* < 0.05. Four embryos from each genotype were measured. (*R*) Quantitative analyses of IHC staining of Myogenin (*I* and *J*), Desmin (*K* and *L*), MHC (*M* and *N*), and Ki-67 (*O* and *P*) in WT skeletal muscle and transformed cells in *aP2-Cre; Ptch1*$^{flox/-}$ mutants (*n* = 4 embryos per genotype). Data are presented as mean ± SD; **P* < 0.05.

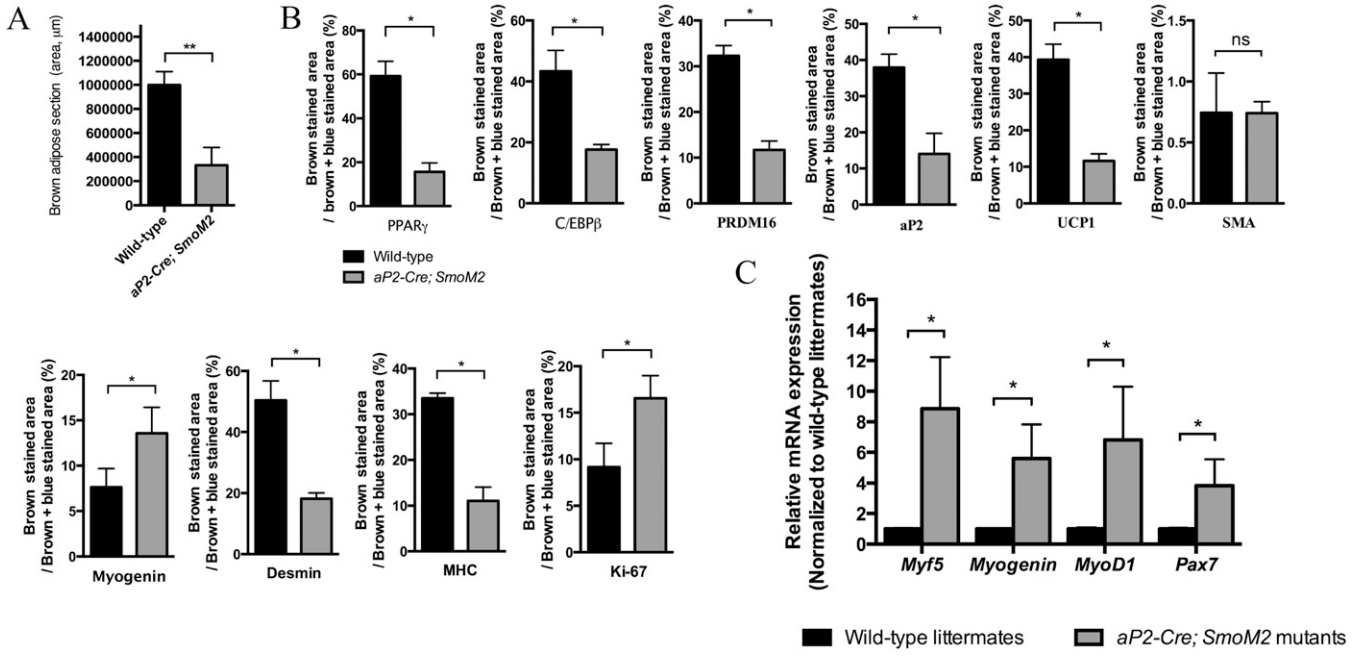

Fig. S4. Quantitative analyses of BAT and phenotypic markers in WT and *aP2-Cre; SmoM2* embryos. (*A*) Comparison of the areas of interscapular BAT observed in sections (Fig. 2 *B* and *C*) from WT and from *aP2-Cre; SmoM2* embryos. Data are presented as mean ± SD; ***P* < 0.01. Four embryos from each genotype were measured. (*B*) Quantification of IHC staining of PPARγ, C/EBPβ, PRDM16, aP2, UCP1, SMA, Myogenin, Desmin, MHC, and Ki-67 in sections from WT and *aP2-Cre; SmoM2* embryos. PPARγ, C/EBPβ, PRDM16, aP2, UCP1, and SMA expression were quantified by comparing images of BAT sections from WT and *aP2-Cre; SmoM2* embryos (Fig. 2 *D–O*) whereas Myogenin, Desmin, MHC, and Ki-67 expression were quantified by comparing skeletal muscle from WT and transformed skeletal muscle from *aP2-Cre; SmoM2* embryos (Fig. 2 *T–A′*) (*n* = 4 embryos per genotype). Data are presented as mean ± SD; **P* < 0.05. (*C*) qRT-PCR analysis to compare expression of the skeletal-muscle progenitor marker genes (*Myf5*, *Myogenin*, *MyoD1*, and *Pax7*) in WT neck BAT (containing both ventral and supraclavicular regions) with expression in the *aP2-Cre; SmoM2* neck BAT (containing transformed cells) (*n* = 4). Data are presented as mean ± SD; **P* < 0.05. The expression of these skeletal muscle markers is greater in the mutants, confirming that these transformed cells indeed resemble skeletal-muscle progenitor cells.

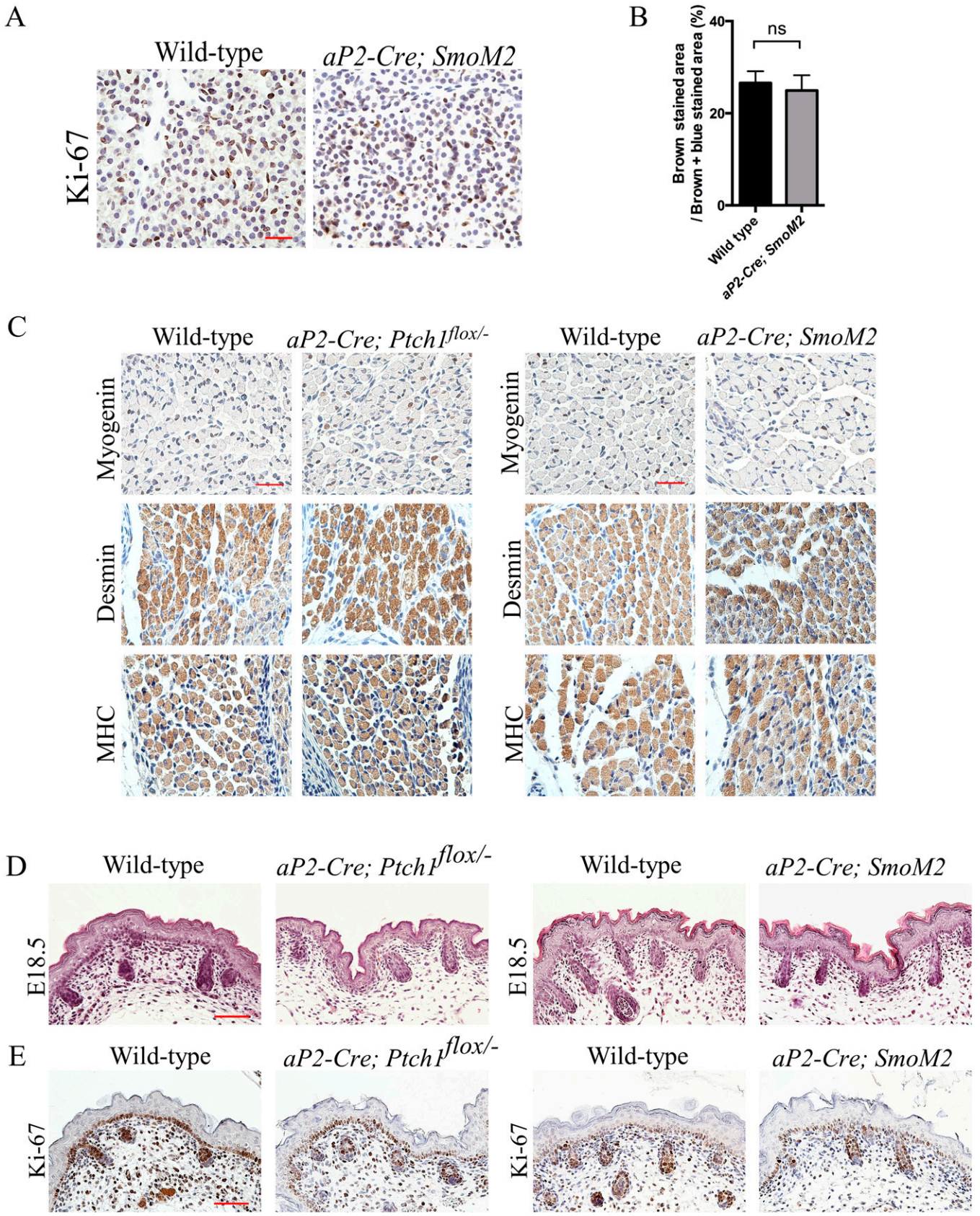

Fig. S5. Brown adipocytes proliferate normally in *aP2-Cre; SmoM2* embryos, and skeletal muscle and dermis develop normally in *aP2-Cre; Ptch1*$^{flox/-}$ and *aP2-Cre; SmoM2* mice. (*A*) IHC of interscapular BAT from E18.5 WT and *aP2-Cre; SmoM2* embryos, using anti– Ki-67 (brown staining). (Scale bar: 25 μm.) (*B*) Quantification of Ki-67–positive staining in E18.5 WT and *aP2-Cre; SmoM2* BAT (n = 3). Data are presented as mean ± SD; ns, nonsignificant. (*C*) IHC of

Legend continued on following page

skeletal muscle adjacent to neck BAT depots from E18.5 WT, *aP2-Cre; Ptch1*$^{flox/-}$, and *aP2-Cre; SmoM2* embryos stained with Myogenin, Desmin, and MHC. (Scale bar: 25 μm.) The expression of these markers and morphology seemed normal in skeletal muscle from these mutants. (*D*) H&E-stained E18.5 WT, *aP2-Cre; Ptch1*$^{flox/-}$, and *aP2-Cre; SmoM2* mouse dermis sections. (Scale bar: 25 μm.) (*E*) IHC of E18.5 WT, *aP2-Cre; Ptch1*$^{flox/-}$, and *aP2-Cre; SmoM2* mouse dermis sections using anti–Ki-67. (Scale bar: 25 μm.) Both H&E and Ki-67 staining showed that dermis seemed normal in WT and mutants.

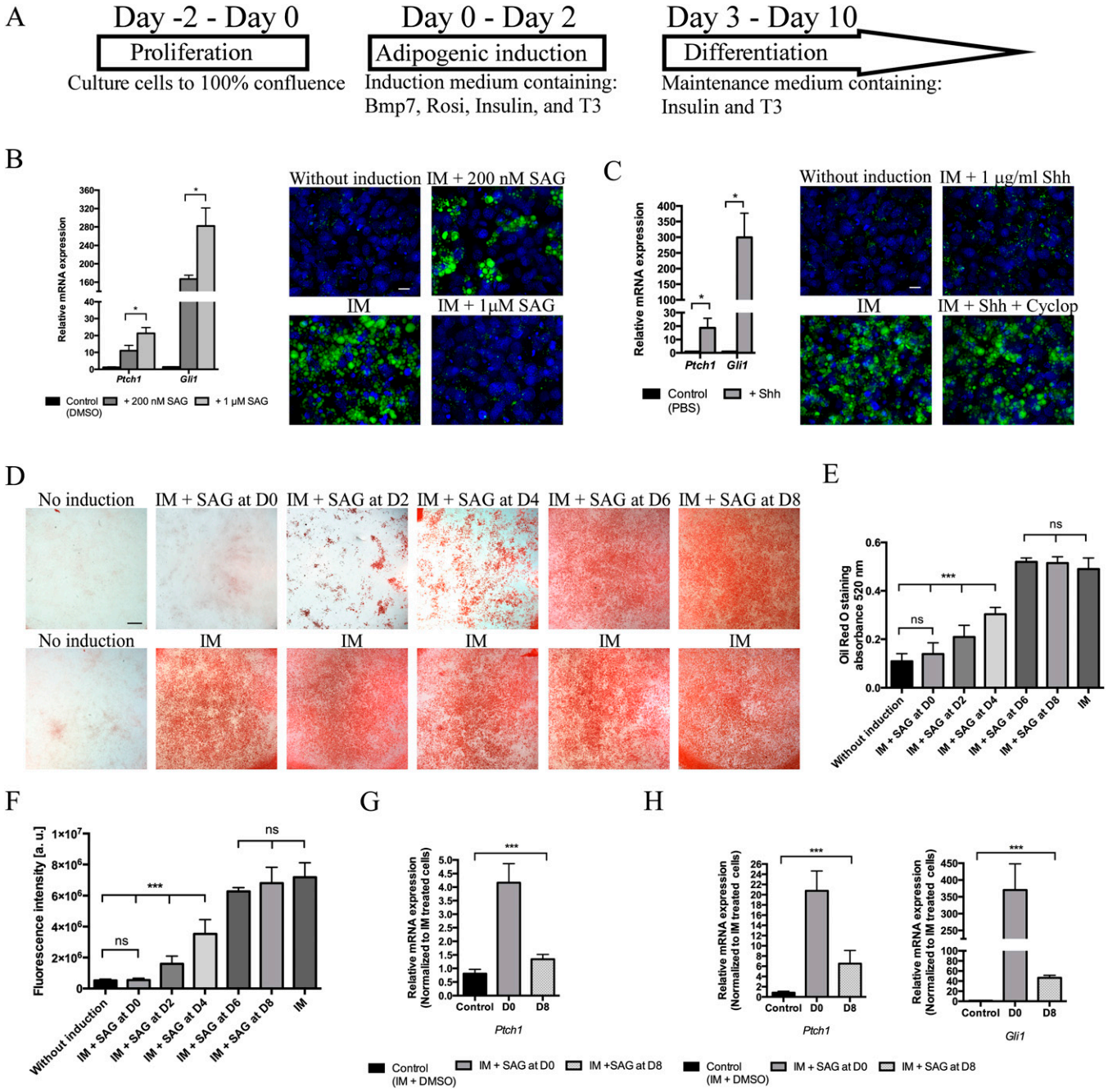

Fig. S6. Brown-preadipocyte differentiation is more sensitive to the inhibitory effect of Hh at earlier stages. (*A*) Scheme describing adipogenic induction conditions used for BAC-C4 differentiation. Briefly, BAC-C4 cells were seeded at 70% confluence (Day –2) and cultured for 2 d until the cells were 100% confluent (Day 0). At day 0, adipogenic induction medium (IM) composed of rhBmp7, Rosiglitazone (Rosi), Insulin, and T3 was added to the culture medium for 2 d (Day 2). After induction, cells were switched to maintenance medium containing Insulin and T3 for another 8 d. (*B*) qRT-PCR analysis of the *Ptch1* and *Gli1* Hh target genes in BAC-C4 cells treated with 200 nM or 1 μM SAG relative to untreated control cells ($n = 3$). Data are presented as mean ± SD; $^*P < 0.05$. The expression of *Ptch1* and *Gli1* is much higher in cells receiving 1 μM SAG. BODIPY staining of lipid droplets in BAC-C4 cells cultured with IM, IM plus 200 nM SAG, or IM plus 1 μM SAG is shown on the *Right*. (Scale bar: 25 μm.) Compared with 1 μM SAG, 200 nM SAG is not very effective at inhibiting brown-preadipocyte differentiation. (*C*) qRT-PCR analysis of *Ptch1* and *Gli1* in BAC-C4 cells treated with 1 μg/mL rShh relative to untreated control cells ($n = 3$). Data are presented as mean ± SD; $^*P < 0.05$. BODIPY staining of lipid droplets in BAC-C4 cells cultured with IM, IM plus Shh, or IM plus Shh plus Cyclop is shown on the *Right*. (Scale bar: 25 μm.) Like cells treated with 1 μM SAG, brown-preadipocyte differentiation is inhibited in BAC-C4 cells treated with 1 μg/mL Shh. (*D*) Oil Red O staining of BAC-C4 cells cultured in IM with or without SAG. SAG was added in 2-d intervals from D0 to D8. Oil red O staining was performed at the end of the 10-d culture period. The accumulation of lipid droplets is largely reduced in cells receiving SAG at early time points, indicating that Hh signaling inhibits early brown preadipocyte differentiation. (Scale bar: 1,000 μm.) (*E*) Quantitative analysis of Oil Red O staining of BAC-C4 cells treated with IM and SAG at 2-d intervals ($n = 4$). Data are presented as mean ± SD; $^{***}P < 0.001$; ns, nonsignificant. (*F*) Quantitative analysis of BODIPY493/503 staining of BAC-C4 cells treated with IM and SAG at 2-d intervals ($n = 4$). Data are presented as mean ± SD; $^{***}P < 0.001$; ns, nonsignificant. Representative images are shown in Fig. 3*G*. (*G*) qRT-PCR analysis of the *Ptch1* Hh target gene in FVB-C3 cells treated with 1μM SAG relative to untreated control cells ($n = 3$). Data are presented as mean ± SD; $^{***}P < 0.001$. D0: SAG was added to the cells at induction of the differentiation process. D8, SAG was added 8 d after induction when cells were nearly terminally differentiated. (*H*) qRT-PCR analysis of the *Ptch1* and *Gli1* Hh target genes in BAC-C4 cells treated with 1μM SAG relative to untreated control cells ($n = 3$). SAG was added as described in *G*. Data are presented as mean ± SD; $^{***}P < 0.001$.

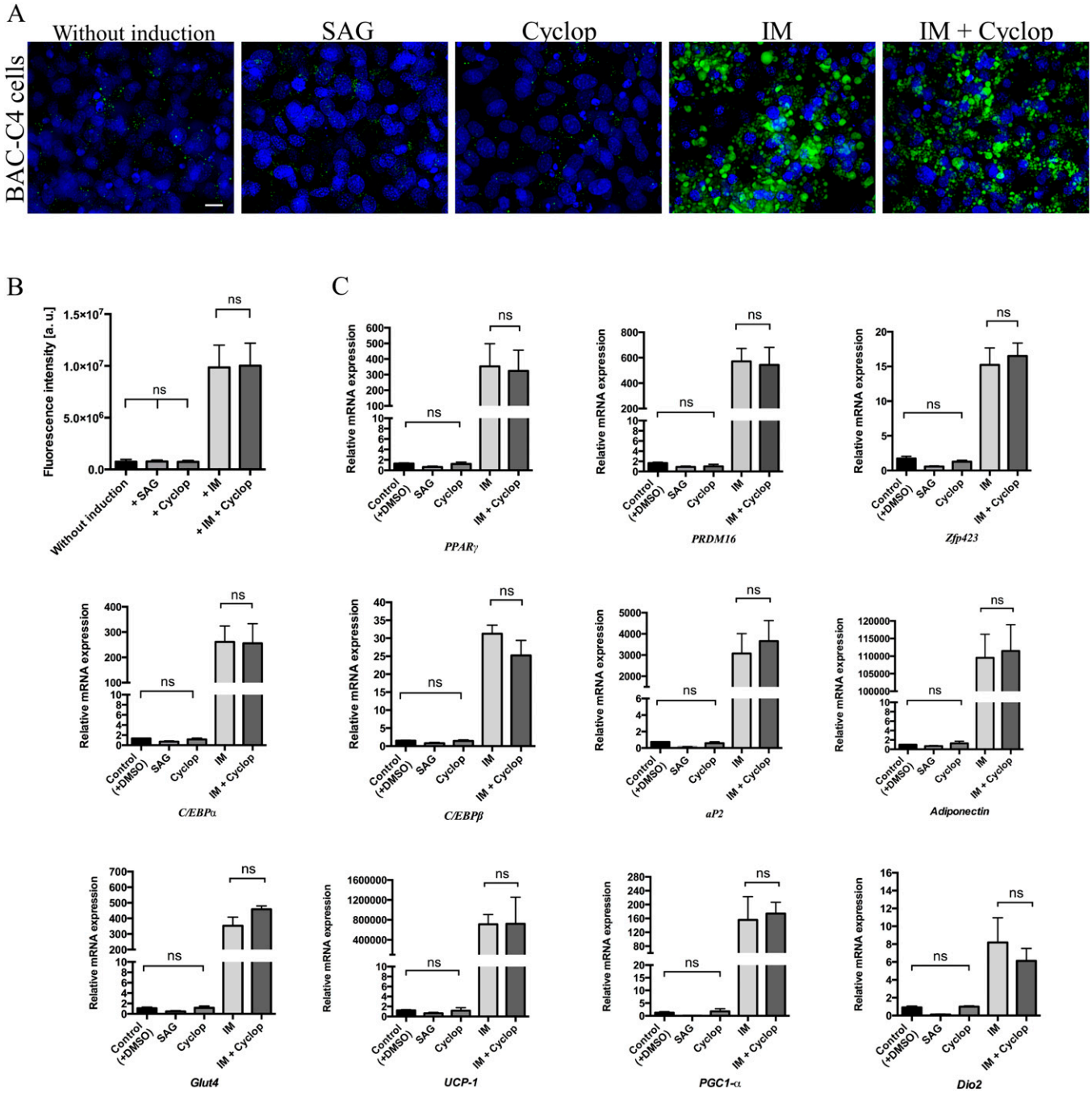

Fig. S7. Cyclopamine alone does not induce or enhance adipogenic differentiation of BAC-C4 cells. (*A*) BODIPY493/503 staining of lipid droplets in BAC-C4 cells cultured with SAG, Cyclop, IM, or IM plus Cyclop. (Scale bar: 25 μm.) (*B*) Quantification of BODIPY493/503 staining of lipid droplets in BAC-C4 cells ($n = 4$). Data are presented as mean ± SD; ns, nonsignificant. (*C*) qRT-PCR analyses of genes involved in brown-preadipocyte differentiation ($n = 3$). Data are presented as mean ± SD; ns, nonsignificant.

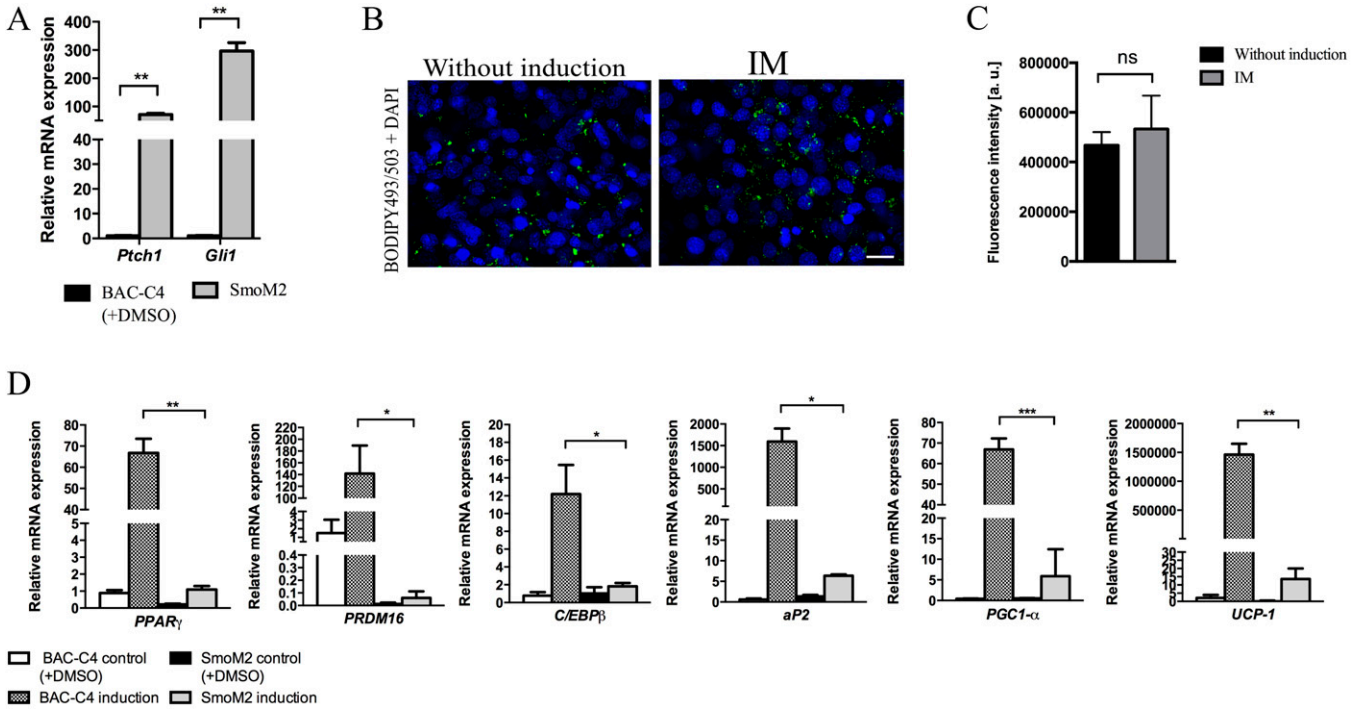

Fig. S8. Hh signaling is autonomously activated in a brown-preadipocyte cell line (designated SmoM2) derived from the interscapular BAT of E16.5 *aP2-Cre; SmoM2* embryos. (*A*) qRT-PCR analyses of two direct Hh target genes, *Ptch1* and *Gli1*. The expression of these two genes was significantly greater in SmoM2 cells than in BAC-C4 cells ($n = 3$). Data are presented as mean ± SD; $^{**}P < 0.01$. (*B*) BODIPY493/503 staining of lipid droplets in untreated SmoM2 cells and SmoM2 cells subjected to the adipogenic differentiation procedure (IM). (Scale bar: 25 μm.) (*C*) Quantitative analysis of BODIPY493/503 staining of SmoM2 cells ($n = 4$). Data are presented as mean ± SD; ns, nonsignificant. (*D*) qRT-PCR analyses of genes involved in brown-preadipocyte differentiation. Compared with WT BAC-C4 cells, expression of adipogenic differentiation markers is significantly reduced in SmoM2 cells ($n = 3$). Data are presented as mean ± SD; $^{***}P < 0.001$, $^{**}P < 0.01$, $^{*}P < 0.05$.

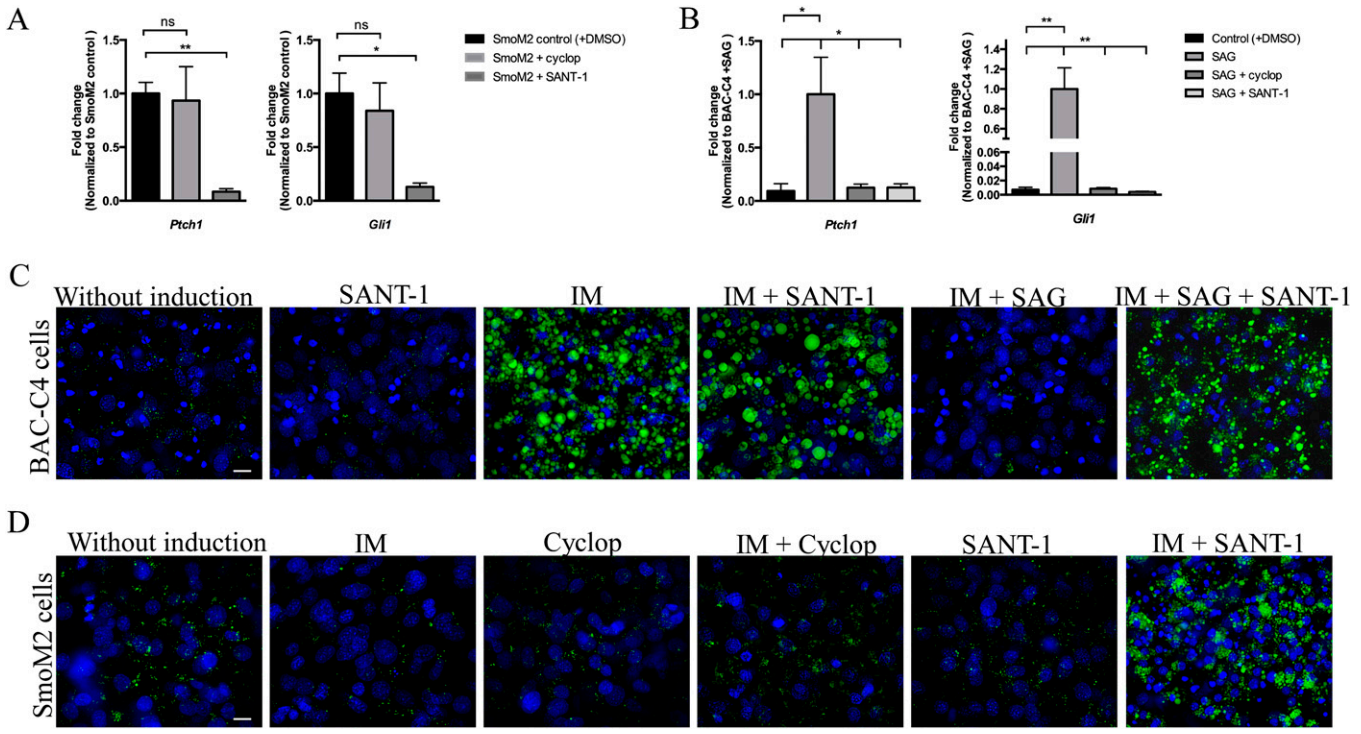

Fig. S9. The Hh-pathway inhibitor, SANT-1, attenuates Hh-pathway activity and reverses the inhibitory effect of Hh on adipogenesis in SmoM2 cells. (*A*) qRT-PCR analyses of *Ptch1* and *Gli1* in SmoM2 cells treated with Cyclop or SANT-1 ($n = 3$). Data are presented as mean ± SD; $^{**}P < 0.01$; $^{*}P < 0.05$; ns, nonsignificant. (*B*) qRT-PCR analyses of two direct Hh target genes, *Ptch1* and *Gli1*, in BAC-C4 cells treated with SAG, SAG plus Cyclop, or SAG plus SANT-1 ($n = 3$). Data are presented as mean ± SD; $^{**}P < 0.01$; $^{*}P < 0.05$. (*C*) BODIPY493/503 staining of lipid droplets in BAC-C4 cells cultured with SANT-1, IM, IM plus SANT-1, IM plus SAG, or IM plus SAG plus SANT-1. (Scale bar: 25 μm.) SANT-1 antagonizes the inhibitory effect of SAG on the differentiation of BAC-C4 cells. (*D*) BODIPY493/503 staining of lipid droplets in SmoM2 cells cultured with IM, Cyclop, IM plus Cyclop, SANT-1, or IM plus SANT-1. (Scale bar: 25 μm.) SmoM2 cells undergo differentiation after treatment with IM plus SANT-1 but not with IM alone or with IM plus Cyclop.

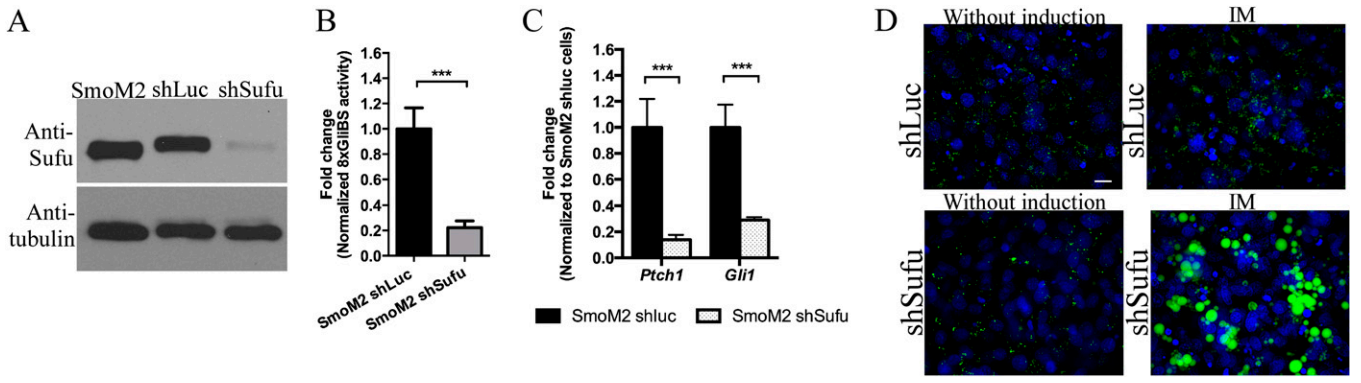

Fig. S10. Knockdown of Suppressor of Fused (Sufu) leads to reduced Hh-pathway activity and restores adipogenic differentiation in SmoM2 brown preadipocyte cells. (*A*) Western blot analysis of Sufu in SmoM2 cells expressing shRNA against *Luciferase* (shLuc, control) and shRNA against *Sufu* (shSufu). (*B*) Hh activity assay using the *8xGliBS-Luc* reporter in SmoM2 cells expressing *shLuc* and *shSufu* ($n = 3$). Data are presented as mean ± SEM; $^{***}P < 0.001$. Hh-pathway activity was reduced in SmoM2 cells expressing *shSufu*. (*C*) qRT-PCR analyses of *Ptch1* and *Gli1* ($n = 3$). Data are presented as mean ± SD; $^{***}P < 0.001$. The expression of these two genes was greatly reduced in SmoM2 cells expressing *shSufu*. (*D*) BODIPY493/503 staining of lipid droplets in SmoM2 cells expressing *shLuc* or *shSufu* and treated with IM. (Scale bar: 25 μm.) SmoM2 cells expressing *shSufu* differentiate after treatment with IM.

Table S1. Primer sequences used for RT-PCR

Gene	Forward sequences (5′–3′)	Reverse sequences (5′–3′)
Shh	GGCCATCTCTGTGATGAACCAGTG	TAGACCCAGTCGAAACCTGCTTCC
Ptch1	GCTATGCTCGCTCTGGAGCACAT	TCAGGACACGGTCCAAAGAAGGAT
Smo	GTTGACTGGGCACAGTGATGATGA	CCACCATCTTGGTGACATGCTGA
Gli1	ACGTGAAGACAGTGCATGGTCCG	AAGGTCCTTCATCCAAGCTGGACA
Gli2	CGTAATGATGTGCATGTCCGTGCT	TCTCCATGCCACTGTCATTGTTGG
Gli3	ACGTGAAGACTGTGCATGGCCC	TGACCACCAGGGCTTGGCTG
β-actin	TGGAATCCTGTGGCATCCATGA	GTACTTGCGCTCAGGAGGAGCAAT

Table S2. Primer sequences used for quantitative RT-PCR

Gene	Forward sequences (5′–3′)	Reverse sequences (5′–3′)
β-Actin	GGCACCACACCTTCTACAATG	GGGGTGTTGAAGGTCTCAAAC
Adiponectin	CGTGATGGCAGAGATGGCACTC	AGCGATACACATAAGCGGCTTCTCC
aP2	ACACCGAGATTTCCTTCAAACTG	CCATCTAGGGTTATGATGCTCTTCA
C/EBPα	AGTACCGGGTACGGCGGGAAC	GCGTGTCCAGTTCACGGCTCA
C/EBPβ	GGACAAGCTGAGCGACGAGTACAAG	TGCTTGAACAAGTTCCGCAGGG
COUP-TFII	TCCAAGAGCAAGTGGAGAAGCTCA	GTACTCTTCCAAAGCACACTGGGACT
Cytochrome C	GGACCAAATCTCCACGGTCTGTTCG	AAATACTCCATCAGGGTATCCTCTCCC
Dio2	TGTGTCTGGAACAGCTTCCTCCTAGA	AAGTCAAGAAGGTGGCATTCGGC
GATA2	ACAAGATGAATGGACAGAACCGGC	ATTGTGCAGCTTGTAGTAGAGGCCAC
GATA3	TATCAAGCCCAAGCGAAGGCTG	GTAGTACAGCCCACAGGCATTGCA
Gli1	CAAGGCCTTTAGCAATGCCAGTGA	ATGCACTGTCTTCACGTGTTTGCG
Glut4	CTGATTCTGCTGCCCTTCTGTCCT	GACATTGGACGCTCTCTCTCCAACTT
Myf5	ATGCCATCCGCTACATTGAGAGC	GACCAGACAGGGCTGTTACATTCAGG
MyoD1	GCACTACAGTGGCGACTCAGATGC	CACTGTAGTCGGTGTCGTAGCC
Myogenin	CATCCAGTACATTGAGCGCCTACAG	GGGAGTTGCATTCACTGGGCAC
Necdin	AGCTCATGTGGTACGTGTTGGTGA	TGTAGCTGCCCATGACCTCTTTCA
NRF-1	TCAGCAAACACAAACTCAGGCCAC	CTGTGGTTGGCAGTTCTGAAGCAT
Pax7	ACAGCTTCTCCAGCTACTCTGACAGCT	CACTCGGGTTGCTAAGGATGCTC
PGC-1α	GTCAACAGCAAAAGCCACAA	TCTGGGGTCAGAGGAAGAGA
PPARγ	AGGGCGATCTTGACAGGAAAGACA	AAATTCGGATGGCCACCTCTTTGC
PRDM16	TCATATGCGAGGTCTGCCACAAGT	TAGTGCTGAACATCTGCCCACAGT
Pref-1	AGTACGAATGCTCCTGCACACCTG	TTGCGGCTACGATCTCACAGAAGT
Ptch1	ACGGTGCTGTGTCCACTCT	CCAGGACGGCAAAGAAGTATC
Ptch1 exon2	TGGTTGTGGGTCTCCTCATATTTGG	TTTAATTCTCGACTCACTCGTCCACC
Runx2	TATGGCGTCAAACAGCCTCTTCAG	TGTTGTTGCTGCTGCTGTTGCT
TFAM	TGGGTATGGAGAAGGAGGCCC	TCATCCTTTGCCTCCTGGAAGC
UCP-1	AGCCACCACAGAAAGCTTGTCAAC	ACAGCTTGGTACGCTTGGATACTG
Wnt10b	GGTGGCTGTAACCACGACATGGA	TGACGTTCCATGGCATTTGCAC
YFP	GAACTTCAAGATCCGCCACAACATC	TGGTAGCTCAGGTAGTGGTTGTCGG
Zpf423	GGCATGGGCGGTACCTTCAAGT	CTTCTGTGGGCACTGCGAGCA

Table S3. Primer sequences used for TaqMan real-time PCR (ChIP analysis)

Region analyzed	
Gli2 ChIP 1: promoter (−3,950 bp to TSS, predicted Gli binding site −3,167 bp to −3,159 bp)	Forward primer: AAATCGTTCGAGCTCTGGCTAT
	Reverse primer: CTGAGGATGTCACCGCACTAAA
	Probe: 6FAM-TGTGTGTGATCAGTAAAT
Negative control	
p16 ChIP 2: promoter (−676 bp to TSS)	Forward primer: GATTGCCCTCCGATGACTTC
	Reverse primer: GTATCAGTGCTAGGATTCTGTACACAACT
	Probe: 6FAM-CCCCGTCACTTTTTTA